Electronic Supplementary Information

For

Magnetic on−off switching in redox non-innocent ligand bridged binuclear cobalt complexes

By

Yichen Wang, [a#] Jing Li, [a#] Li Zhang, [a] Chao Chen, [a] Rui Feng, [a] Yi-Quan Zhang,[b] Gengwen Tan*[a]
You Song *[a] and Xinping Wang *[a]

[a]*State Key Laboratory of Coordination Chemistry, School of Chemistry and Chemical Engineering, Collaborative Innovation Center of Advanced Microstructures, Nanjing University, Nanjing 210023, China*

Email: gengwentan@nju.edu.cn; yousong@nju.edu.cn; xpwang@nju.edu.cn

[b]*Jiangsu Key Laboratory for NSLSCS, School of Physical Science and Technology, Nanjing Normal University, Nanjing 210023 (China)*

Email: zhangyiquan@njnu.edu.cn

# These two authors contribute equally to this work.

Content

Experimental Part

General considerations: All experiments were carried out under a moisture-free nitrogen or argon atmosphere by using standard Schlenk or glove box techniques. All solvents were dried by standard methods and freshly distilled before used. UV-vis spectra were recorded on Lambda 750 spectrometer. Elemental analyses were performed at Shanghai Institute of Organic Chemistry, the Chinese Academy of Sciences. The temperature-dependent magnetic data for polycrystalline samples was collected on a Quantum Design MPMP-XL7 superconducting quantum interference device (SQUID) magnetometer, while the field-dependent magnetization and alternative-current properties were measured on a MPMS Squid VSM. For the single crystal X-ray structure analyses, the crystals were each mounted on a glass capillary in perfluorinated oil and measured in a cold N_2 flow. The data were collected on Bruker D8 CMOS detectors at 123K. The structures were solved by direct methods and all refined on F^2 with the SHELX-2014/2018 software package. The positions of the H atoms were calculated and considered isotropically according to a riding model. Commercially available reagents were purchased from Aldrich, Acros or Alfa-Assar, and used upon arrival. LCo(Tol)[1] and $[Cp_2Fe][BPh_4]$[2] were synthesized according to the literature method.

Synthesis of 1: LCo(Tol) (200 mg, 0.35 mmol) and 2,2'-bipyrimidine (26.5 mg, 0.17 mmol) was placed in a Schlenk flask (100 mL), and toluene (30 mL) was added *via* cannula. The mixture was stirred at room temperature overnight. After filtration, the filtrate was concentrated in vacuo to afford dark brown solid of **1**. Yield: 97 mg, 48.5%. X-ray quality crystals were grown by slowly cooling a warm THF solution to room temperature. Elemental analysis for $C_{66}H_{88}N_8Co_2$(%): Calculated: C 71.33, N 10.08, H 7.98; Found: C 71.64, N 10.32, H 7.97. IR (KBr, cm^{-1}): 685.0, 758.6, 794.1, 1021.5, 1086.6, 1100.0, 1141.0, 1176.6, 1261.1, 1316.0, 1390.6, 1435.9, 1462.2, 1519.9, 2866.0, 2925.5, 2961.0, 3056.9. UV-Vis (THF, nm): 331.

Synthesis of 2: LCo(Tol) (200 mg, 0.35 mmol) and 2,2'-bipyrimidine (26.5 mg, 0.17 mmol) was placed in a Schlenk flask (100 mL), and toluene (30 mL) was added *via* cannula. The mixture was stirred at room temperature overnight. After removel of solvent in vacuo, $[Cp_2Fe][BPh_4]$ (90 mg, 0.18 mmol) was added, then fluorobenzene (30 mL) was added *via* cannula and stirred at room temperature for 1 day. The solution was filtered and the filtrate was then concentrated. Minimum hexane (2 mL) was added to afford dark brown solid of **2**. Yield: 73 mg, 36.5%. X-ray quality crystals were grown by layering a concentrated THF solution with hexane. IR (KBr, cm^{-1}): 669.8, 682.3, 713.8, 759.5, 759.1, 838.5, 885.7, 935.2, 1127.7, 1163.3, 1278.2, 1355.1, 1437.7, 1463.7, 1558.5, 2872.6, 2932.3, 2969.7. UV-Vis (THF, nm): 328.

Table S1. Crystal Data and Structure Refinement for **1** and **2**[a]

	1	**2**
formula	$C_{66}H_{88}Co_2N_8$	$C_{94}H_{116}BCo_2N_8O$
formula weight	1111.30	1502.61
crystal system	monoclinic	Triclinic
space group	$P21/n$	P-1
a/Å	12.577(2)	15.2751(6)
b/Å	16.039(3)	16.3305(6)
c/Å	15.838(2)	20.2692(7)
α/deg		84.7460(10)
β/deg	105.293(4)	76.3530(10)
γ/deg		72.5170(10)
V/Å^3	3081.9(8)	4685.3(3)
Z	2	2
ρ_{calcd}/g·cm^{-3}	1.198	1.065
μ/mm^{-1}	0.583	0.400
F(000)	1188	1606
crystal size/mm^3	0.20 x 0.15 x 0.10	0.27 x 0.25 x 0.19
θ range/deg	2.242–25.00	2.068–25.0009
index ranges	$-24 \leq h \leq 14$	$-18 \leq h \leq 16$
	$-18 \leq k \leq 19$	$-19 \leq k \leq 14$
	$-18 \leq l \leq 18$	$-24 \leq l \leq 24$
collected data	19966	34490
unique data	5405 (R_{int} = 0.0674)	16458 (R_{int} = 0.0299)
completeness to θ	99.8%	99.6%
data/restraints/parameters	5405 / 0 / 353	16458 / 191 / 1020
GOF on F^2	1.011	1.037
final R indices [I>2σ(I)]	R_1 = 0.0441 wR_2 = 0.0875	R_1 = 0.0412 wR_2 = 0.1017
R indices (all data)	R_1 = 0.0786 wR_2 = 0.1019	R_1 = 0.0582 wR_2 = 0.1111
Largest diff peak/hole (e·Å^{-3})	0.303/–0.239	0.268/–0.302

[a] All data were collected at 123(2) K using Mo K$_\alpha$ (λ = 0.71073 Å) radiation. $R_1 = \sum(||F_o| - |F_c||)/\sum|F_o|$, $wR_2 = \{\sum[w(F_o^2 - F_c^2)^2/\sum[w(F_o^2)^2]]\}^2\}^{1/2}$, GOF = $\{\sum[w(F_o^2 - F_c^2)^2]/(N_o - N_p)\}^{1/2}$.

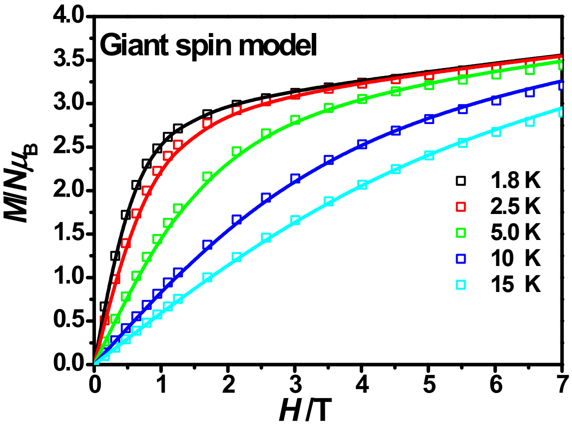

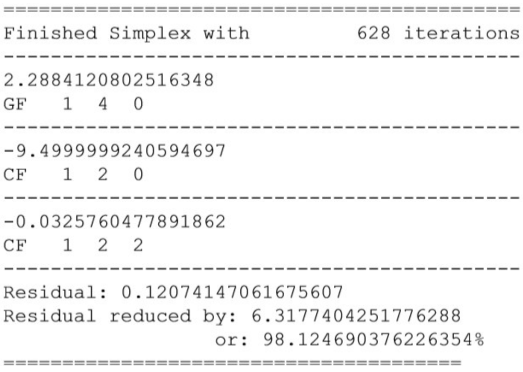
```
============================================
Finished Simplex with         628 iterations
--------------------------------------------
2.2884120802516348
GF   1  4  0
--------------------------------------------
-9.4999999240594697
CF   1  2  0
--------------------------------------------
-0.03257604778918 62
CF   1  2  2
--------------------------------------------
Residual: 0.12074147061675607
Residual reduced by: 6.3177404251776288
                  or: 98.124690376226354%
=======================================
```

Fig. S1 The fitting result of *M*-*H* with giant spin model of **2**.

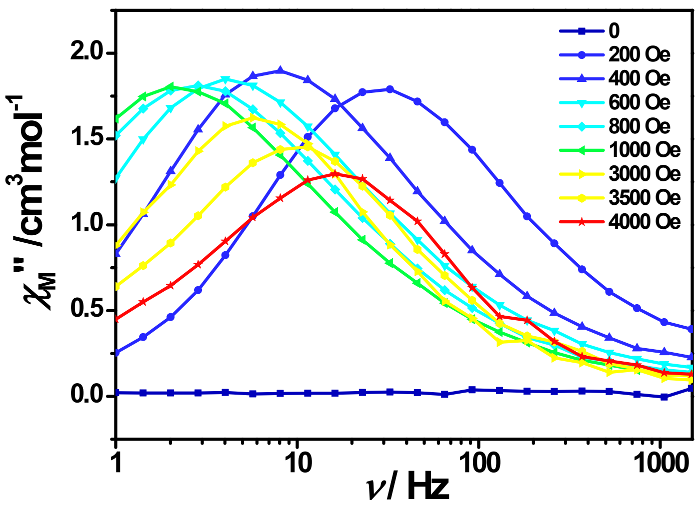

Fig. S2 The frequency-dependence out-of-phase (χ'') AC magnetization susceptibility of **2** with different dc field at 1.8 K.

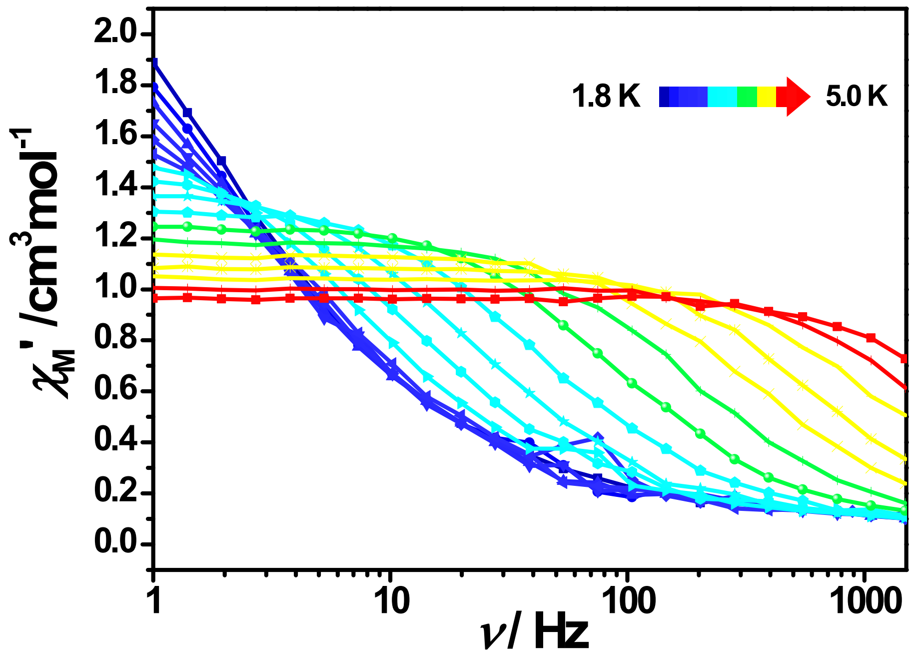

Fig. S3 The frequency-dependence in-phase (χ′) AC magnetization susceptibility of **2** under 1.0 kOe in the temperature range of 1.8 – 5.0 K.

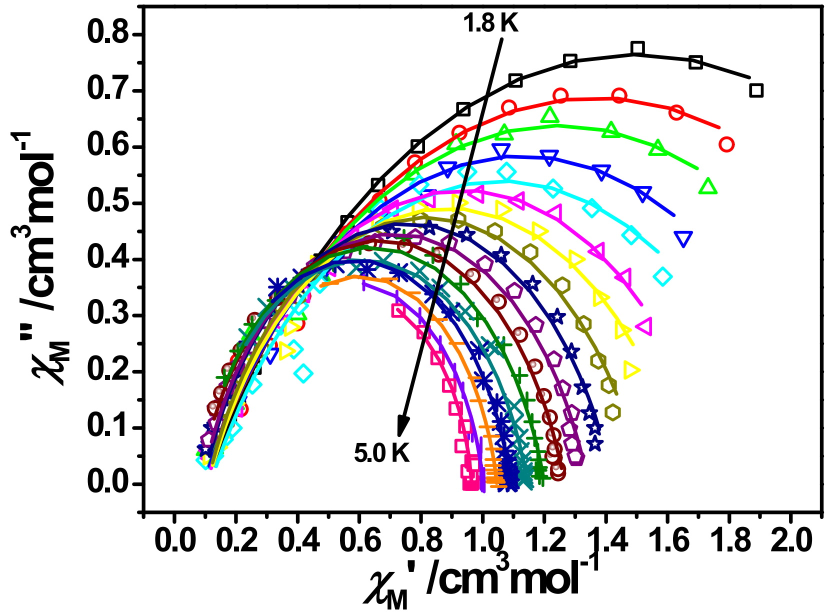

Fig. S4 Cole-cole plot of **2** under 1.0 kOe in the temperature range of 1.8 – 5.0 K.

Ab initio calculations for complexes 1 and 2

Both of binuclear complexes **1** and **2** have an inversion center, thus only one individual Co^{II} fragment was calculated, respectively. Complete-active-space self-consistent field (CASSCF) calculations on individual Co^{II} fragments of the model structures (see Fig. S5 for the calculated model structure of complexes **1** and **2**) extracted from the compounds on the basis of single-crystal X-ray determined geometry have been carried out with MOLCAS 8.2 program package.[3] Each individual Co^{II} fragment was calculated keeping the experimentally determined structure of the corresponding compound while replacing the neighboring Co^{II} ion by diamagnetic Zn^{II}. In the calculation of individual Co^{II} fragment of complex **2**, the spin of the central radical was considered as 0.

The basis sets for all atoms are atomic natural orbitals from the MOLCAS ANO-RCC library: ANO-RCC-VTZP for Co^{II} ions; VTZ for close N; VDZ for distant atoms. The calculations employed the second order Douglas-Kroll-Hess Hamiltonian, where scalar relativistic contractions were taken into account in the basis set and the spin-orbit couplings were handled separately in the restricted active space state interaction (RASSI-SO) procedure. For the calculation of Co^{II} fragments, active electrons in 10 active spaces considering the 3*d*-double shell effect (5+5′) include all seven 3*d* electrons (CAS(7 in 5+5′)), and the mixed spin-free states (all from 10 quadruplets and 20 from 40 doublets). Single_Aniso[4] program was used to obtain the energy levels, ***g*** tensors, m_J values, magnetic axes, *et al.,* based on the above CASSCF/RASSI calculations.

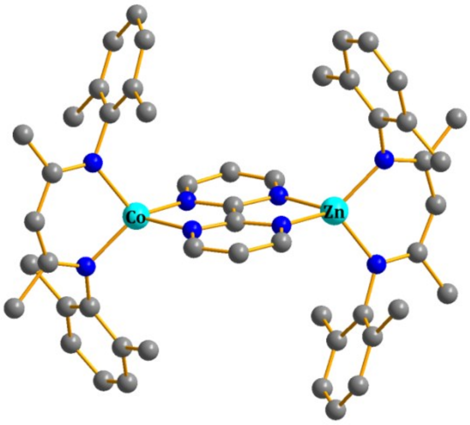

Fig. S5 Calculated model structure of individual Co^{II} fragment of complex **1** and **2**; H atoms are omitted.

Table S2. Calculated zero-field splitting parameters D (E) (cm^{-1}) and $\boldsymbol{g}$ (g_x, g_y, g_z) tensor of the lowest spin-orbit state of individual Co^{II} fragment of complexes **1** and **2** using CASSCF/RASSI with MOLCAS 8.2.

[1]		**[1]$^+$**	
D (E)	$\boldsymbol{g}$	D (E)	$\boldsymbol{g}$
−28.0 (2.7)	2.131 2.186 2.511	−29.2 (2.8)	2.122 2.177 2.526

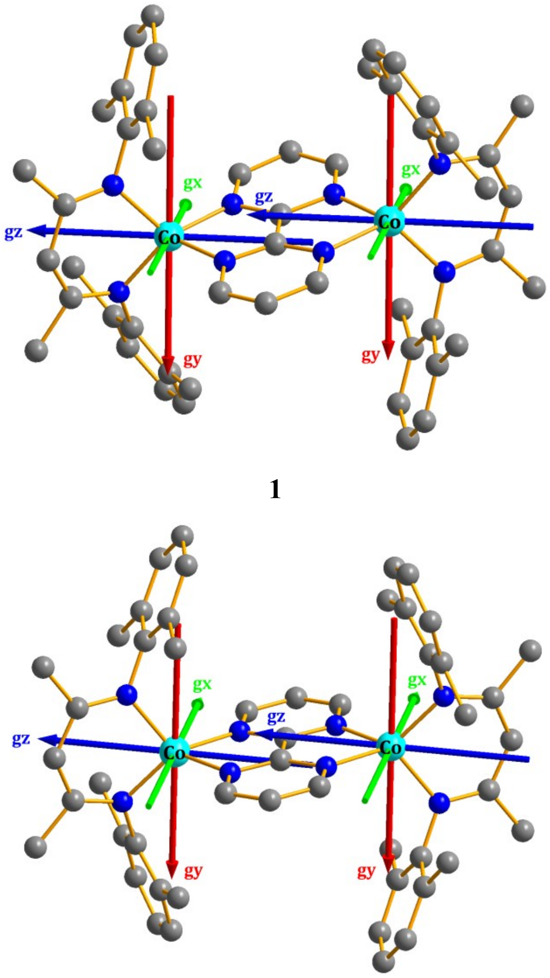

1

2

Fig. S6 Orientations of the local magnetic axes of the ground doublet on Co^{II} ions of complexes **1** and **2** using CASSCF/RASSI with MOLCAS 8.2.

The calculated *D, E* (cm^{-1}) and ***g*** tensor (*x, y, z*) of individual $\mathrm{Co^{II}}$ fragments of complexes **1** and **2** using CASSCF/RASSI were listed in Table S2 where the calculated *D* values of two complexes are both negative and similar. The calculated orientations of the ***g*** tensors on $\mathrm{Co^{II}}$ ions of complexes **1** and **2** were shown in Fig. S6.

Estimation of the exchange interactions by BS-DFT calculation

To obtain the isotropic exchange coupling constants *J*, Orca 4.0.1 calculations[5] were performed with the popular hybrid functional B3LYP proposed by Becke[6-7] and Lee et al.[8] Triple-ζ with one polarization function TZVP[9-10] basis sets were used for all atoms, and scalar relativistic Hamiltonians (ZORA) was used for the scalar relativistic effect in all calculations. For complex **2**, only the nearest neighboring Co^{II}-Radical exchange interactions were considered. The calculated model structure including one radical and two Co^{II} was shown in Fig. S7.

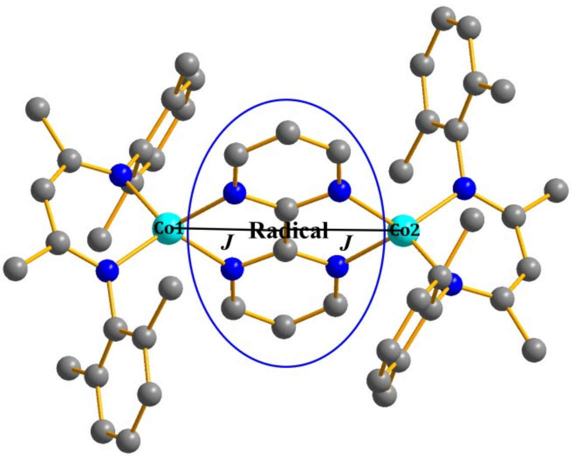

Fig. S7 Calculated model structure of the labeled exchange coupling constants for complex **2**; H atoms are omitted.

There is only one type of *J* between Co^{II} and radicals. The large integration grid (grid = 5) was applied to Co^{II} for ZORA calculations. Tight convergence criteria were selected to ensure the results to be well converged with respect to technical parameters. Through calculating the energies of two spin states: the high-spin state ($S_{HS} = S_{Co1}+S_{Radical}+S_{Co2}$), the low-spin state (flip the spins on Radical; $S_{LS} = S_{Co1}-S_{Radical}+S_{Co2}$), the isotropic Co^{II}-Radical coupling constant $J_{Co\text{-}Rad}$ was obtained as eq. 1 using the spin-projected approach[11-13] according to the Heisenberg exchange Hamiltonian: $\hat{H} = -2J_{Co-Rad}(S_{Co1}S_{Rad} + S_{Co2}S_{Rad})$

$$J_{Co-Rad} = \frac{E_{LS} - E_{HS}}{8} \qquad (1)$$

The calculated Co^{II}-Radical coupling constant $J_{Co\text{-}Rad}$ using eq 1 is -114.5 cm^{-1}, which shows that the antiferromagnetic interactions between Co^{II} and radicals are very strong. Ruiz and coworkers[14] showed that self-interaction error within B3LYP-BS approach could overestimate the exchange coupling constant. And so, they proposed the spin non-projected approach[15] combined with

B3LYP-BS method to evaluate *J*. They showed that such approach could give more accurate *J* values compared to the experiments for a lot of transition metal complexes.[14] The isotropic Co^{II}-Radical coupling constant $J_{Co\text{-}Rad}$ was obtained as eq. 2 using the non-projected approach.[15]

$$J_{Co-Rad} = \frac{E_{LS} - E_{HS}}{12} \qquad (2)$$

The calculated Co^{II}-Radical coupling constant $J_{Co\text{-}Rad}$ using eq 2 is −76.3 cm^{-1}.

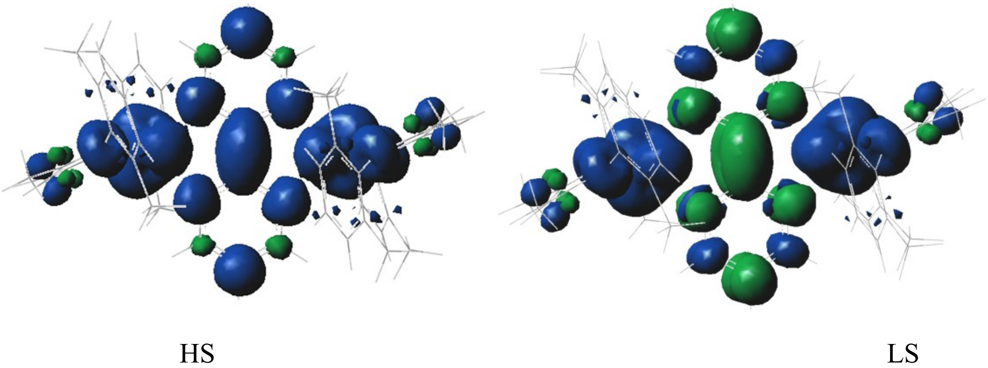

Fig. S8 Spin density distribution map of complex **2** in the high (left) and low (right)-spin state (blue and green regions indicate positive and negative spin populations, respectively; the isodensity surface represented corresponds to a value of 0.002 e^{-} bohr^{-3}).

References:

(1) Spitzer, F.; Graßl, C.; Balázs, G.; Mädl, E.; Keilwerth, M.; Zolnhofer, E.M.; Meyer, K.; Scheer, M. *Chem. Eur. J.*, 2017, **23**, 2716.

(2) Piglosiewicz, I. M.; Beckhaus, R.; Wittstock, G.; Saak, W.; Haase, D. *Inorg. Chem.*, 2007, **46**, 7610.

(3) (a) Aquilante, F.; De Vico, L.; Ferré, N.; Ghigo, G.; Malmqvist, P.-Å.; Neogrády, P.; Pedersen, T. B.; Pitonak, M.; Reiher, M.; Roos, B. O.; Serrano-Andrés, L.; Urban, M.; Veryazov, V.; Lindh, R. *J. Comput. Chem*., **2010**, *31*, 224. (b) Veryazov, V.; Widmark, P. -O.; Serrano-Andres, L.; Lindh, R.; Roos, B. O. *Int. J. Quantum Chem*., **2004**, *100*, 626. (c) Karlström, G.; Lindh, R.; Malmqvist, P. -Å.; Roos, B. O.; Ryde, U.; Veryazov, V.; Widmark, P. -O.; Cossi, M.; Schimmelpfennig, B.; Neogr´ady, P.; Seijo, L. *Comput. Mater. Sci*., **2003**, *28*, 222.

(4) (a) Chibotaru, L. F.; Ungur, L.; Soncini, A. *Angew. Chem. Int. Ed.*, **2008**, *47*, 4126. (b) Ungur, L.; Van den Heuvel, W.; Chibotaru, L. F. *New J. Chem.*, **2009**, *33*, 1224. (c) Chibotaru, L. F.; Ungur, L.; Aronica, C.; Elmoll, H.; Pilet, G.; Luneau, D. *J. Am. Chem. Soc.*, **2008**, *130*, 12445.

(5) (a) Neese, F. ORCA–an ab initio, density functional and semiempirical program package, version 4.0.1; Max-Planck institute for bioinorganic chemistry: Mülheim an der Ruhr, Germany, 2017. (b) Neese, F. *WIREs Comput. Mol. Sci.* **2018**, *8*: e1327. doi: 10.1002/wcms.1327.

(6) Becke, A. D. *J. Chem. Phys*. **1993**, *98*, 5648.

(7) Becke, A. D. *Phys. Rev. A*. **1988**, *38*, 3098.

(8) Lee, C.; Yang, W.; Parr, R. G. *Phys. Rev. B*. **1988**, *37*, 785.

(9) Schafer, A.; Horn, H.; Ahlrichs, R. *J. Chem. Phys*. **1992**, *97*, 2571.

(10) Schafer, A.; Huber, C.; Ahlrichs, R. *J. Chem. Phys.* **1994**, *100*, 5829.

(11) Noodleman, L. *J. Chem. Phys*. **1981**, *74*, 5737.

(12) Noodleman, L.; Baerends, E. J. *J. Am. Chem. Soc.* **1984**, *106*, 2316.

(13) Noodleman, L.; Case, D. A. *Adv. Inorg. Chem*. **1992**, *38*, 423.

(14) Ruiz, E.; Alvarez, S.; Cano, J.; Polo, V. *J. Chem. Phys*. **2005**, *123*, 164110.

(15) Ruiz, E.; Rodriguez-Fortea, A.; Cano, J.; Alvarez, S.; Alemany, P. *J. Comput. Chem*. **2003**, *24*, 982.